

# Exploration of methylation changes during transformation and evaluation as circulatory pre-cancer markers during tumorigenesis

## Abstract

Epigenetics with aberrant DNA methylation is an early event in cancer development, and recent research is mainly focused on cancer-specific DNA methylations and their clinical utility in cancer detection and management. In the current study, methylation patterns of 18 overexpressed genes were observed in the cellular model (A16 and NA16) and in the circulation of tumorigenic mice to determine whether these methylation changes occur concurrently during transformation/ tumorigenesis. The results from the present study showed an enhancement of DNMT activity to 4-fold in transformed rat fibroblast cell lines in their non-adherent condition at the 16h time period. However, methylation analysis revealed only two genes out of 18, namely HIF1A and VEGFA, were amplified as methylated and unmethylated successively in both control and transformed cells. Upon transplantation into Nude mice, we observed the release of methylated HK2 and unmethylated VEGFA into the blood circulation of tumorigenic mice from weeks 1 to 11. The results confirm that HK2 & VEGFA may serve as methylated/unmethylated markers in the non-invasive detection of cancer at an early stage.

**Keywords:** cancer, transformed cells, tumorigenic mice, DNMTs, DNA methylation, methylated markers

## Introduction

Cancer is a multifactorial disease driven by genetic and epigenetic changes characterized by six hallmark properties such as self-sufficiency in growth signals, insensitivity to growth-proof signals, evasion from apoptosis, unlimited replicative possibilities, continued angiogenesis, tissue invasion and metastasis.<sup>1,2</sup> Recent research suggests that the accumulation of genetic and epigenetic alterations in the normal cell genome can lead to the malignant transformation of normal cells.<sup>3</sup> Transformed cells can form neoplastic phenotypes and perform key transitions required for tumor initiation and early tumorigenesis.<sup>4</sup> Epigenetic modifications play a significant role in understanding the complexities of cancer biology.<sup>1</sup> Epigenetics is a series of biological processes involving DNA methylation, histone modifications, and chromatin remodeling.<sup>5</sup> DNA methylation involves the covalent transfer of a methyl group to the C-5 position of the cytosine residues in a CpG dinucleotide of the promoter region by DNA methyltransferases (DNMTs).<sup>6</sup> Abnormal methylation patterns as one of the prominent epigenetic hallmarks of cancer, playing a critical role in cancer initiation, progression, therapy responses, and therapy resistance.<sup>7</sup> Hyper methylation of promoters and hypo methylation of global DNA are quite common in tumorigenesis. These changes occur in the promoters of tumor suppressors and oncogenes, leading to silencing and activation, respectively.<sup>8</sup>

Methylation patterns of gene promoters in circulating DNA represent similar alterations in tumor tissue genomic DNA and the tumor microenvironment.<sup>8</sup> These methylation patterns can be detected through liquid biopsy, such as circulating DNA (ctDNA), offering a non-invasive method to assess tumor-specific alterations in blood-derived DNA and monitor early cancer development. Gene promoters involved in abnormal methylations during the early stages of tumorigenesis may serve as potential markers for tumor screening,

prognosis assessment, evaluation of therapeutic efficacy, and personalized treatment. The important cancer-specific changes that can give information about premalignancy or malignant conditions are aberrant promoter methylations in the circulating DNA.<sup>9</sup>

Epigenetic gene regulation has a significant impact on an organism's growth and development.<sup>10</sup> Several FDA-approved methylated biomarkers are used for cancer detection. One of the most prominent methylated biomarkers till now is the Hyper methylation of *SEPT9* or *SFRP2* in colorectal carcinoma (CRC) diagnosis.<sup>11</sup>

Our previous study demonstrated that a subset of fibroblasts can resist anoikis during late stages, acquiring transformation-associated properties such as anchorage-independent growth, *in vitro* colony formation in soft agar, and *in vivo* tumor formation in nude mice. Cytogenetic analysis revealed the presence of a t (2;2), and several cancer-related genes were upregulated.<sup>3,12,13</sup> Based on microarray data, 18 overexpressed genes related to hypoxia, glycolysis, and tumor progression were selected for further exploration as circulatory tumor markers.

Hypoxia-inducible factor 1-alpha (HIF-1-alpha), Vascular endothelial growth factor A (VEGF A), Hexokinase 2 (HK2), DNA damage-inducible transcript 3 (DDIT3), Epidermal growth factor receptor (EGFR), 3-phosphoinositide-dependent protein kinase-1 (PDK1), Solute Carrier Family 2 Member A (SLC2A), Secreted phosphoprotein 1 (SPP1), Matrix metalloproteinase-3 (MMP3), Retinoblastoma protein (RB1), Egl nine homolog 3 (EGLN3), Stanniocalcin 1 (STC1), 6-phosphofructokinase (PFKM), Alcohol dehydrogenase 1 (ADH1), Aldehyde dehydrogenase 3A1 (ALDH3A1) genes were analyzed for abnormal promoter methylation patterns in A16 and NA16 cells and also in the circulation of tumorigenic mice.

## Materials and methods

### Cell culture

Rat fibroblast cell line F111 used in the present study was a generous gift from Dr. Gopal Pande, Center for Cell and Molecular Biology, Hyderabad. The cells were grown in Dulbecco's modified Eagle medium (DMEM) containing 10 % Fetal Calf Serum (FCS), penicillin (100 U/ml), and streptomycin (50 mg/ml) at 37°C with 5% CO<sub>2</sub> and 95% relative humidity.

### Preparation of transformed cells from F111 cell line

F111 cells were trypsinized at 70-80% confluent and suspended in complete DMEM. 5X10<sup>6</sup> cells were plated on a 0.8 % agarose-coated surface, and another set plated on a plastic surface was incubated at 37°C with 5% CO<sub>2</sub>. After 16hr time period, cells collected from plastic surfaces were labeled as "Adherent (A16)/Control" cells, and those collected from agarose surfaces were labeled as "Nonadherent (NA16)/Transformed".<sup>3</sup> Transformed cell phenotype was confirmed by observing morphological properties like cytoskeletal organization and anchorage-independent growth according to the methods suggested by Jinka et al.<sup>3</sup> The cells were suspended in cold Phosphate-buffered saline (PBS) for further use.

### Cell viability test

MTT (3-(4,5-dimethylthiazol-2-yl)-2,5-diphenyl tetrazolium bromide) assay was performed to confirm the cell viability as described in Kumar et al.<sup>14</sup>

### DNA methyltransferase (DNMT) activity in transformed cells

DNMT activity assay was performed in nuclear extracts collected from 5X10<sup>6</sup> Adherent (A16) and non-adherent (NA16) cells. The cells were suspended in cold PBS were lysed with buffer A (50 mM HEPES (pH 7.4), 1 mM EGTA, 1 mM EDTA, 19 mM KCl, 1 mM DTT, and 0.025% NP-40 with proteo-block (10 µl/ml) and the cell mixture was incubated on ice with the intermittent vortex for 30 minutes. After vertexing, the mixture was centrifuged at 4,000 g for 10 min, pellet was collected and washed 3 times with buffer "A". To the washed pellet buffer "B" (50 mM HEPES (pH 7.4), 1 mM EDTA, 400 mM KCl, 1 mM EGTA, 0.5 percent Triton X-100, 1 mM DTT and proteo-block solution (10 µl/ml)) was added and kept at 4°C for 30 minutes on the rotor. The mixture was centrifuged at 14,000 rpm for 10 min, and the supernatant was considered a nuclear fraction.<sup>15</sup> DNMT activity in the nuclear fraction was calorimetrically measured at 450 nm according to the manufacturer's instructions for EpiQuik™ DNMT Activity/Inhibition Assay Ultra Kit (Colorimetric) purchased from Epigen Tek, Farmingdale, NY, USA.

DNMT activity [(OD at 450nm)/ (h·mg)] was calculated using the following formula:

$$\text{DNMT activity} = (\text{No of inhibitor OD} - \text{Blank OD}) / (\text{Protein Amount} (\mu\text{g}) \times \text{hours}) \times 1000$$

### Tumorigenesis by using transformed cells

Homozygous nude mice (NIH strain, Nu/Nu) aged between 4 - 6 weeks and weighing 20g) were purchased from Vivo Bio Tech Pvt., Ltd. (Hyderabad, India) and were kept in Animal Care Facilities without specific pathogens. In the current study, a total of 16 mice were used for *in-vivo* animal experiments. Mice were randomly assigned to 2 groups consisting of 8 animals with equal numbers of males and females and acclimatized for 2 weeks to the laboratory

conditions. Blood samples were obtained from each animal in each group before the transplantation of transformed cells by the retro-orbital method. 5×10<sup>6</sup> A16 and NA16 cells collected in PBS were transplanted subcutaneously into homozygous nude mice of 4 - 6 weeks to generate tumors in a gradation manner for the period of 3 months. The tumor volume was measured every week, and at the same time, 100µl blood was drawn to examine the methylation status of selected genes during the period of early tumorigenesis.<sup>3</sup>

### Isolation of DNA

**From transformed cells:** DNA from both A16 and NA16 cells was extracted by using a TRIzol reagent according to the manufacturer's protocol.<sup>16</sup> Isolated DNA was precipitated from the interphase by adding 150 µl of 100% ethanol and centrifuged at 2000 g for 5 min at 4°C. The pellet was washed twice with 500 µl of 10% ethanol in 0.1 mol/l sodium citrate and resuspended in 30 µl TE buffer (1 M Tris-HCl, pH 7.6, 2 ml 0.5 M EDTA, pH 8).

**From the circulatory blood of tumorigenic mice:** DNA was isolated from 100µl of circulatory blood collected from the tumorigenic mice by following a standard protocol with few changes.<sup>17</sup> 150 µl of red cell lysis buffer (0.01 M Tris-HCl, pH 7.6, 320 mM sucrose, 5 mM MgCl<sub>2</sub>, and 1% Triton X 100) was added to 100 µl blood and homogenized by gentle mixing. White blood cells (WBC) and hemoglobin were cleared by repeated washings with a red cell lysis buffer. The mixture was centrifuged at 7,000 rpm for 2 min to collect the pellet, and then 200-400µl of nucleic acid lysis buffer (0.01 M Tris-HCl, pH 7.5, 11.4 mM Sodium citrate, 1 mM EDTA, 1% SDS) was added. To the resulting mixture, saturated NaCl (5M) and 600µl of chloroform were added and centrifuged at 7,000 rpm for 2 minutes. The supernatant was precipitated by adding cold absolute ethanol and re-centrifuged at 12,000 rpm for one minute. The pellet was resuspended in a TE buffer and stored at 4°C until future use. DNA concentration was determined using the Nanodrop.<sup>18</sup> Animal experiments were conducted according to the approval of the ethical committee of CSIR-IICT, Hyderabad (IAEC; protocol number: IICT/08/2018).

### Bisulfite conversion and purification

Isolated DNA was chemically modified and treated with sodium bisulfite to convert unmethylated cytosine into uracil, while the methylated cytosine remained unchanged. DNA collected from A16, NA16, and tumorigenic animals were subjected to sodium bisulfite conversion.<sup>19</sup> Briefly, the DNA was incubated with 0.2 M NaOH at 37°C for 10 min and further with freshly prepared 10 mM of hydroquinone (Sigma) and 3M of sodium bisulfite (Sigma), and the mixture was incubated at 50°C for 16 hours by overlaying with mineral oil. Modified DNA was purified by using the DNA purification resin (Bio serve) and eluted into 50µl of water and stored at -20 °C.

### Identification of CpG islands

CpG islands in selected genes were identified by the Methprimer Database. The identified CpG islands have a GC content of more than 50% and a ratio of observed CpG/expected CpG greater than 0.6. All the identified CpG islands are within 1500 nucleotides upstream of the transcription start site.

### Designing of Primers at the promoter for the selected genes

Primers were designed to perform Methylation-specific PCR (MSP) for the genes HIF1A, VEGF-A, HK2, DDIT2, EGFR, SLC2A1, and PDK1 selected based on their upregulation in glycolysis/glycogenesis, and hypoxia pathways based on microarray data

while transforming in NA16 cells.<sup>3</sup> The remaining 11 genes with no CpG islands were detected in PFKM, ADH1, ALDH3A1, SPP1, MMP3, RB1, EGLN3, STC1, MMP3, CD133, and ABCG-2. The promoter sequence was retrieved by locating the TSS (Transcription Start Site) position with the help of the Database of Transcriptional Start Sites (DBTSS) and Eukaryotic Promoter Database (EPD). CpG islands were identified in the promoter sequence and the primers were designed by using MethPrimer: <http://www.urogene.org/methprimer/index1.html>. All primers were synthesized at Bioserve Biotechnologies (India) Private Ltd., located in Hyderabad, Telangana.

### Methylation-specific PCR

Methylation patterns of the genes (HIF1A, VEGF-A, HK2, DDIT2, EGFR, SLC2A1, and PDK1) at the Promoter region were analyzed using an MSP-based technique.<sup>20-22</sup> 20  $\mu$ l reaction mixture that contained 50ng of bisulfite-modified DNA, 1 X PCR buffer (Takara) 2.5 mm of MgCl<sub>2</sub> except for Hif1 $\alpha$  (1.5 mm), deoxyribonucleotide triphosphate (dNTP) each at 1.25 mM, 200 nm of forward primer, 300 m of reverse primer except for EGFR (200 nm) and HIF 1 $\alpha$  (400 nm), 0.5 U of Hot-Star Taq DNA polymerase (Qiagen) was prepared and amplified in a temperature cycler with an activation step of 7 min at 95°C, followed by 40 cycles of 30 s at 95°C, 30 s at annealing temperature, 30 s at 72°C extension step; followed by a final 4-min extension at 72°C. For each set of PCRs, controls without DNA were performed. For Hif1 $\alpha$ , nested PCR was performed by using the amplified product of the previous MSP reaction as a template under the same PCR conditions. The amplified PCR product was run through 2% agarose gel.

### Calculation of band intensity

Intensities of the DNA bands on the agarose gels were analyzed using ImageJ software, NIH, USA. Gel images were first loaded into the software, and all the images were made in 8-bit grayscale. The image was then inverted to enhance the resolution of the bands. The region of interest (ROI) was drawn around each lane using a rectangle tool, and the lanes were selected using the “Analyse > Gels > Select Lanes” option. The lane intensity profiles were obtained by selecting “Plot Lanes,” which produced graphical representations of the bands. For all the quantification of the areas of the bands, the line tool was used to draw the baseline of each peak in the intensity plot, and then the magic wand tool was used to measure the area under each peak. The area under a peak was automatically detected by this tool for each band peak’s intensity. The “Label Peaks” function was used to calculate the percentage of area occupied by every band with regard to total lane intensity. The outcome was the determination of these values, and the percentage’s relative intensity was recorded and exported to Microsoft Excel for later handling. This led to normalizing the relative band intensities by dividing the intensity of each band from the highest percent value of the dataset.

## Results

### Cell viability test

The viability of control and transformed (A16 and NA16) cells was confirmed with the regular MTT assay. The results were concurrent with the previous study observed in Jinka et al.<sup>3</sup>

### DNA methylase transferase activity in control and transformed cells

The activity of DNA methyl transferases was assessed in control and transformed cells as it is responsible for the maintenance and changes in DNA methylation during the process of tumorigenesis. It

was observed that DNMT activity is enhanced while transforming and observed to be 165 $\pm$ 0.9 units/h/mg in NA16 cells when compared to that of control adherent, A16 cells, where it was found to be 40 $\pm$ 0.5 units/h/ $\mu$ g. The results indicated an increase in DNMT activity to 4-fold during transformation, shown in Figure 1.

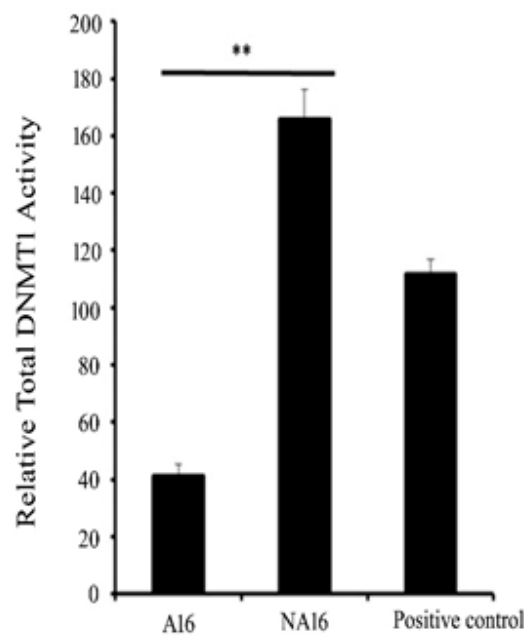


**Figure 1** The Standard deviation bar graph represents DNMT Activity in Control (A16) and Transformed Cells (NA16). The standard deviation is calculated from the average of three individual experiments.

\*\*denotes a statistically significant difference between control and transformed cells ( $p < 0.01$ ). Error bars represent standard deviation.”

### Tumorigenesis by using control and transformed cells

Control (A16) and transformed (NA16) cells were implanted subcutaneously into the 6–8-week-old homozygous nude mice (Nu/Nu) to generate tumors and observe the methylation/unmethylation patterns of selected genes in the circulatory blood of tumorigenic mice.  $5 \times 10^6$  cells, each from control and transformed cells, were administered subcutaneously, and the tumor growth was measured at week intervals up to 11 weeks. The results for tumorigenesis were concurrent with a previous study,<sup>3</sup> where control cells did not induce any tumor, however, it was observed the initiation of tumors from the 4<sup>th</sup> week onwards grew gradually to a size of 240 mm<sup>3</sup> at the 11<sup>th</sup> week. 100 $\mu$ l of circulatory blood was drawn to study for the circulatory tumor markers for a 0–11 week time period.

Primarily, the study is focused on methylated markers to detect the cancer at the early stage. 50–100 ng DNA was collected from the 100  $\mu$ l of circulatory blood of control and tumorigenic animals and subjected to bisulfite conversion. The concentration of DNA isolated from blood is 50 ng/ $\mu$ l. The concentration of DNA extracted from control and transformed cells is 178 ng/ $\mu$ l and 80 ng/ $\mu$ l, respectively. After the bisulfite conversion, a reduction in the concentration of DNA from 34% - 46% was observed.

### Retrieval of the gene promoter for the methylation status

The results clearly showed that only 7 genes (HIF1A, VEGF-A, HK2, DDIT2, EGFR, SLC2A1, and PDK1) out of 18 have CpG

islands (Table 1), and the remaining 11 genes (Adh1, MMP3, MMP9, MMP10, EGLN3, PFKM, ALDH3A1, CD133, SPP1, RB1, and STC1 genes) did not show any CpG islands.

**Table I** Number of CpG islands in the promoter regions and fold change values of transformed cells and tumorigenic animals. Fold change data in cells and tumors are adapted from Jinka et al.<sup>3</sup>

S. No	Gene name	No of CpG islands	Fold change cells	Fold change tumor
1	HIF1A	1	NC	2.08
2	VEGFA	3	-2.5	NC
3	HK2	3	4.78	NC
4	DDIT3	2	8.45	4.64
5	EGFR	2	2.43	NC
6	SLC2A1	1	5.8	2.11
7	PDK1	2	9.11	-2.75

### Methylation-specific PCR in *in vitro* and *in vivo* conditions

The methylation changes of CpG islands of 5 genes were studied using methylation-specific PCR after bisulfite conversion in both transplanted cells and circulatory blood of animals to explore the differences in the methylation patterns of selected genes *in vitro* and *in vivo* conditions. The MSP results for HIF1 $\alpha$  showed the appearance of methylated HIF1A in control cells and appeared to be partially methylated (methylated & unmethylated) in transformed cells (Figure 2). The corresponding bands were quantified in the ImageJ software, the results are shown in Table SI. The quantification results revealed that the unmethylated HIF1A band intensity with 1.0 was decreased in transformed cells to a value of 0.740341. In contrast, an increased methylation of the gene with an intensity of 0.288053 was observed in transformed cells. The result indicates that the partial demethylation of methylated DNA in control cells is a consequence of the change during transformation. However, there was no amplification of HIF1A either in methylated/unmethylated state in the circulation of the control and tumorigenic animals was observed.

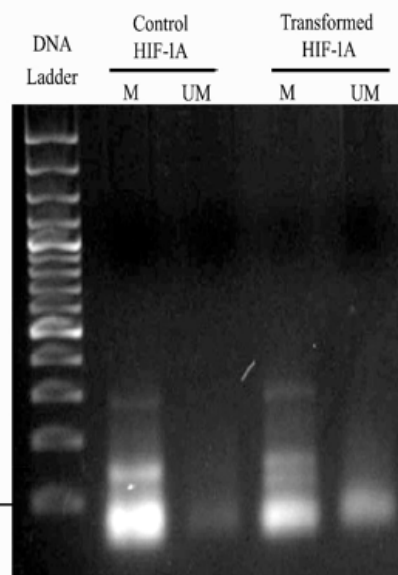


**Figure 2** 2% agarose gel of MSP PCR product of HIF1A in control and transformed cells. The above figure illustrates Lane 1 150 bp DNA ladder, Lane 2, intensified Methylated HIF1A in control cells, Lane 3, Faintest unmethylated HIF1A in control cells, Lane 4, intense thick methylated HIF1A in transformed cells, Lane 5, slightly visible unmethylated HIF1A in transformed cells.

**Table SI** Band intensities of HIF1A in control and transformed cells

Methylation status	Band intensity	Band intensity
	(Control)	(Transformed)
Unmethylated	1	0.740341
Methylated	0.028394	0.288053

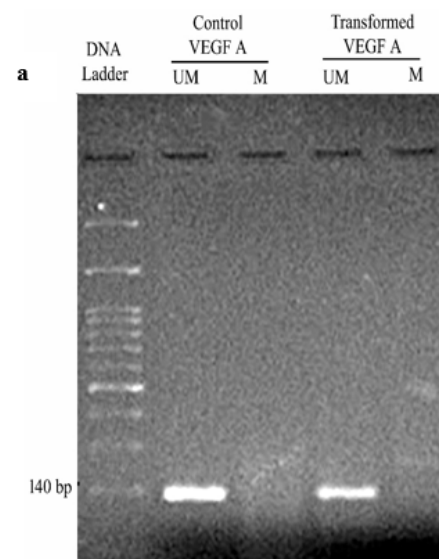
Similarly, the MSP for VEGFA, as shown in Figures 3a and 3b, clearly revealed the presence of unmethylated VEGFA in both cell conditions (Control and transformed). The band intensity showed no difference for unmethylated amplicons of product size 140 bp (Table SII). When injected into the nude mice, unmethylated VEGFA appeared in the blood circulation from weeks 1 to 11. The results from the band intensities showed elevated levels up to 1.3547 in the tumorigenic animal when compared to the control animal (Table SIII).

**Table SII** Band intensities of VEGFA in control and transformed cells

Methylation status	Band intensity	Band intensity
	(Control)	(Transformed)
Unmethylated	1	1.003965
Methylated	0.086189	0.082225

**Table SIII** Band intensities of VEGFA in control and tumorigenic mice

Week no	Band intensity	Band intensity	Band intensity	Band intensity
	(Control)	(Control)	(Tumor)	(Tumor)
Week 0	0.056638	0	0.045161	0
Week 1	0.140849	0	0.263158	0
Week 2	0.520951	0	0.45236	0
Week 3	0.69725	0	0.230492	0
Week 4	0.515857	0	0.389474	0
Week 5	0.581868	0	1.024652	0
Week 6	0.781392	0	0.756944	0
Week 7	0.276876	0	0.641969	0
Week 8	0.441358	0	0.374805	0
Week 9	0.921154	0	0.698744	0
Week 10	0.85691	0	1.354703	0
Week 11	1	0	0.558778	0



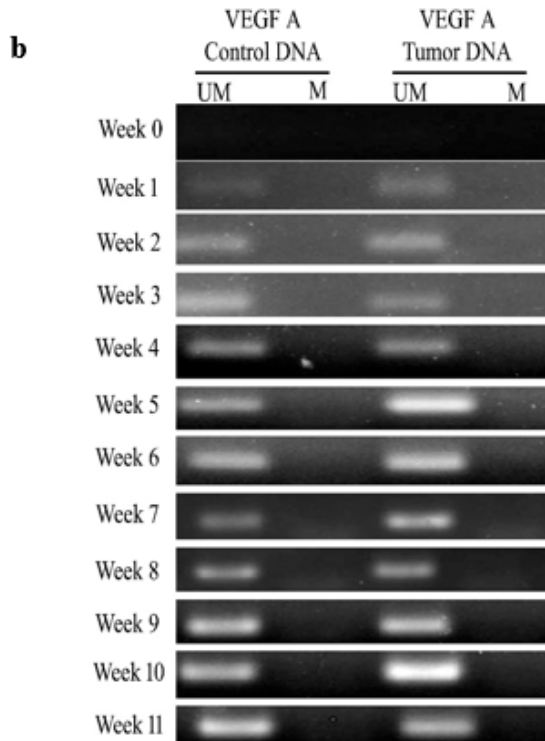


**Figure 3** (a and b) 2% agarose gel of MSP PCR product of VEGFA in cells and animal models. (a) 3a represents Lane 1 of 150 bp DNA ladder, Lane 2, unmethylated VEGFA amplicon in control cells, Lane 3, No amplicon is observed, Lane 4 unmethylated VEGFA amplicon in transformed cells, Lane 5, No amplicon was observed. (b) Figure 3b describes the week-wise analysis (Week 0 - Week 11) of the release of unmethylated VEGFA in control and tumorigenic nude mice.

HK2 gene is not amplified either in methylated/unmethylated conditions in control and transformed cells, however, it is amplified in the blood circulation of both control and tumorigenic animals in unmethylated form. HK2 was released into the blood circulation from week 1 to week 11, with a gradual increase up to week 5, and then decreased, indicating the low concentration of template DNA in the circulation. In contrast, methylated HK2 was released into the circulation in the first week and increased gradually during the 5<sup>th</sup> week of the tumorigenesis (Figure 4). In both conditions, the maximum intensity of 1.0 was observed in the 5<sup>th</sup> week (Table SIV). The result indicated that a high concentration of unmethylated HK2 released in the control is modified into a methylated form in tumorigenic mice during the latent period of tumor generation (4 weeks).

**Table SIV** Band intensities of HK2 in control and tumorigenic mice

Week	Band intensity	Band intensity	Band intensity	Band intensity
	(Control)	(Control)	(Tumor)	(Tumor)
	UMa	Mb	UMa	Mb
Week 0	0.003286	0	0	0
Week 1	0.115078	0	0	0.037152
Week 2	0.746335	0	0	0.428277
Week 3	1.030776	0	0	0.544892
Week 4	0.913043	0	0	0.013416
Week 5	I	0	0	I

Week 6	0.755056	0	0	0.293086
Week 7	0.732305	0	0	0.794634
Week 8	0.805675	0	0	0.035088
Week 9	0.07457	0	0	0.184727
Week 10	0.064585	0	0	0.211558
Week 11	0.078741	0	0	0.052632

<sup>a</sup>UM -Unmethylated, <sup>b</sup>M -Methylated

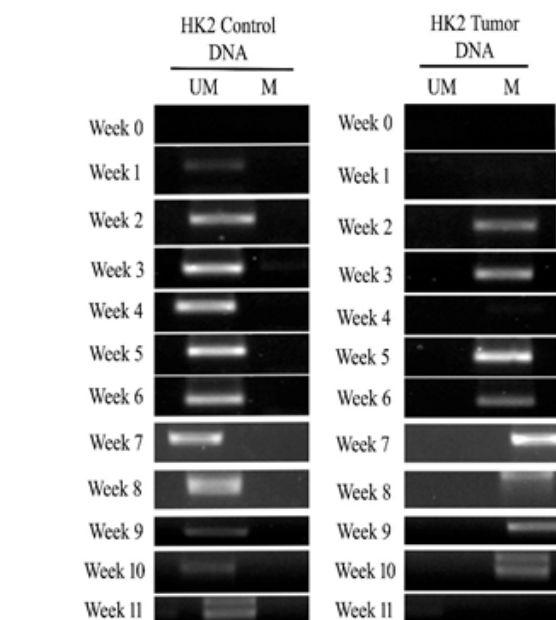


**Figure 4** 2% agarose gel of MSP PCR product of HK2 in control and tumorigenic animals. Week-wise analysis of release of unmethylated HK2 in control animals and methylated HK2 in tumorigenic animals.

MSP results of DDIT3 showed the release of unmethylated DDIT3 from the fourth week in control animals and the fifth week in tumor animals, though it is not amplified in transplanted cells (Figure 5). The band intensity analysis in ImageJ software revealed that both animals showed maximum intensity level of 1.0 in week 5 (Table SV). In control animals, a gradual increase in intensity was observed up to the 5<sup>th</sup> week and declined further. In tumorigenic animals, no change was observed initially up to the 4<sup>th</sup> week, and a prominent dark band was observed with maximum intensity during week 5, and it decreased at a later period to 1.

**Table SV** Band intensities of DDIT3 in control and tumorigenic mice

Week no	Band intensity	Band intensity	Band intensity	Band intensity
	(Control) UMa	(Control) Mb	Tumor UMa	Tumor Mb
Week 0	0.341463	0	0.082011	0
Week 4	0.810421	0	0.042328	0
Week 5	I	0	I	0
Week 6	0.988914	0	0.449735	0
Week 7	0.249446	0	0.164021	0
Week 8	0.160754	0	0.140212	0
Week 9	0.198448	0	0.055556	0
Week 10	0.029933	0	0.121693	0
Week 11	0.124169	0	0.042328	0

<sup>a</sup>UM -Unmethylated, <sup>b</sup>M -Methylated

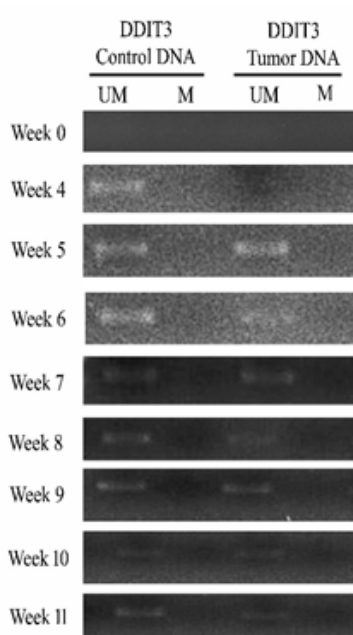


**Figure 5** 2% agarose gel of MSP PCR product of DDIT3 in control and tumorigenic animals. Week-wise analysis of the release of unmethylated DDIT3 in control and tumorigenic nude mice.

It was observed that methylated EGFR was released into the circulation from 6<sup>th</sup> to 11<sup>th</sup> week in both control and tumorigenic animals (Figure 6). The band intensity results showed maximum intensity 1.0 at week 10 in both control and tumorigenic animals (Table SVI). However, the amplification level in the circulation for the gene was progressive in control and tumorigenic animals.

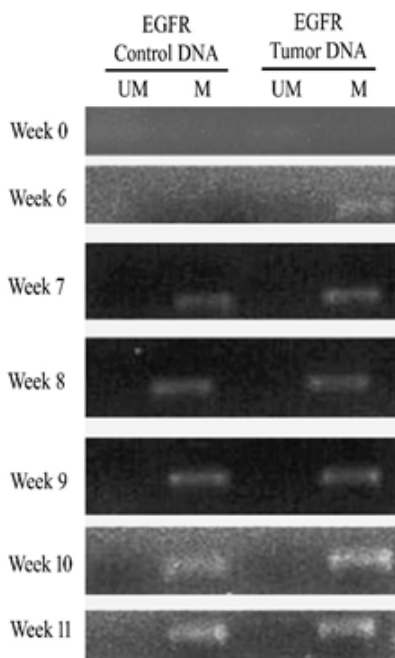


**Figure 6** 2% agarose gel of MSP PCR product of EGFR in control and tumorigenic animals. Week-wise analysis of the release of methylated EGFR in control and tumorigenic nude mice.

**Table SVI** Band intensities of EGFR in control and tumorigenic mice

Week no	Band intensity	Band intensity	Band intensity	Band intensity
	(Control) UMa	(Control) Mb	Tumor UMa	Tumor Mb
Week 0	0	0.060051	0	0.029472
Week 6	0	0.117762	0	0.275206
Week 7	0	0.286712	0	0.375151
Week 8	0	0.686697	0	0.289095
Week 9	0	0.76931	0	0.427227
Week 10	0	1	0	1
Week 11	0	0.916619	0	0.629751

<sup>a</sup>UM -Unmethylated, <sup>b</sup>M -Methylated

## Discussion

DNA methylation is an essential epigenetic mechanism observed in the CpG island of promoter regions that influences a wide range of biological functions, including transcription activity, chromatin organization, imprinting, cellular differentiation, and chromosome stability.<sup>23</sup> Detecting aberrant DNA methylation status of different targeted genes in circulating tumor DNA (ctDNA) has been proposed as a promising biomarker for the early diagnosis and monitoring of cancer.<sup>24</sup> The aberrant methylation events that occurred in the promoter regions of specific genes in tumor tissue were reflected in the circulating tumor DNA, which is released from tumor tissue either through apoptosis or necrosis of tumor cells. It was reported the existence of circulating tumor DNA (ctDNA) derived from tumor cells in the body fluids such as peripheral blood, urine, saliva, or sputum.<sup>25</sup> Most circulating DNA arises from leukocytes, and some ctDNA alterations that might appear to be cancer-derived actually arise from leukocytes with clonal hematopoiesis or other abnormalities.<sup>26</sup> The elevated concentrations of cfDNA represented in the circulation of cancer patients would be from the neoplastic cells and the surrounding non-neoplastic epithelial cells.<sup>27</sup> The current work has represented the changes in the methylation pattern of the genes HIF1A, VEGFA, HK2, DDIT3, and EGFR selected based on microarray observations in normal and transformed cells, based on the existence of CpG islands and their release into the blood circulation of tumorigenic mice when transplanted into nude mice.

As described earlier the results of cell viability were consistent with the previous findings and the cells attained transforming/tumorigenic properties at 16-hour time period by gaining all the hallmark properties of cancer cells with elevated proliferative signaling, resistance to cell death, copious to angiogenesis and capable to induce tumors and metastasize at different sites when injected into Nude mice.<sup>3</sup> Abnormal changes in DNA methylation have been reported in a variety of tumors, including both hematological malignancies and solid tumors.<sup>28</sup> Assessing epigenetic changes in the genome of tumors and body fluids provides an overview of changes in the tumor microenvironment.

Epigenetic modification at the identified CpG islands of HK2, HIF1 $\alpha$ , DDIT3, VEGF A, and EGFR genes was studied by using primers (Table 2) designed in a bioinformatic-based search engine Metprimer. Variations in CpG islands from 1 to 3 were observed at their promoter regions for the represented genes. DNA methylation changes of several genes have been observed in various cancers and are considered significant biomarkers in carcinogenesis detection.<sup>29-31</sup> DNMT activity is a major enzyme responsible for epigenetic changes

and is observed to be aberrant in the process of tumorigenesis.<sup>32</sup> An increase in 4-folds of DNMT activity in transformed cells indicated that the enzyme may be responsible for the changes in the genome of transformed cells and correlated with up/down-regulation of genes, playing a role in the progression of tumors and consistent with

previous reports in different types of cancer.<sup>33</sup> The aberrant activity of DNMTs significantly affects cancer progression by hypermethylation of tumor suppressor genes (TSGs) and hypomethylation of proto-oncogenes.<sup>28</sup>

**Table 2** Primers specific for the methylated and unmethylated regions of selected genes

Primer set	Sense primer,* 5' 3'	Antisense primer,* 5' > 3'	Annea temp., °C
PDK1 Ma	TAGGTTTATTGTTAAGGATTTCGT	AAATCCAACCTAAACTATATCGCA	49
PDK1 UMb	GATAGGTTTATTGTTAAGGATTTGT	AAAATCCAACCTAAACTATATCACA	50
HK2 M	TGGAGTTTGGGTTTAGTTAC	TATACGCTCTCCGACTACCC	51
HK2 UM	TGGAGTTTGGGTTTAGTTAT	TATACACTCTCCAACCTACCC	50
SLC2a1 M	TTCGTTTTTCGTTAGAATTACGT	ACTACCTTTTATAAAACCGCCG	50
SLC2a1 UM	TTTGTGTTTTGTTAGAATTATGT	ACTACCTTTTATAAAACCAACCACC	51
HIF1α M	TAGTCGGAGGAGTAATTAGGAATTC	AAATCCAAAACGAAATATAAAACG	48
HIF1α UM	TTGGAGGAGTAATTAGGAATTGGA	ATCCAAAACAAAATATAAAACAAA	51
DDIT3 M	TTAGTATTTTTATTATTATCGACGT	ATAACTTTAAATCAGGAAACTTCGC	51
DDIT3 UM	TTAGTATTTTTATTATTATGTGATGT	AACTTTAAATCACAAAACCTTCACA	47
VEGFA M	CGTAGAGGTTGGGTAGTC	AATCCGTTAAATAATCTACCTTATCG	52
VEGFA UM	AGAAAGTGTAGAGGTTGGGTAGTT	AATCCATTAAATAATCTACCTTACT	51
EGFR M	GACGTTGGATAGTTTAGCGTAAC	CGTCGCCTATCTAATAACGAT	51
EGFR UM	TGTTTGGATAGTTTAGTGTAAATGT	ACCCATCACCTATCTAATAACAAAT	49

<sup>a</sup>M -Methylated <sup>b</sup> UM -Unmethylated

DNA methylation is a relatively stable biochemical modification carried out by DNA methyltransferases. Variations in the epigenetic modifications caused by DNMT in HK2, HIF1α, DDIT3, VEGF A, and EGFR genes were assessed in transformed cells and the blood circulation of tumorigenic animals at weekly intervals by bisulfite conversion and Methylation-specific PCR.

HIF-1A is a gene responsible for the regulation of cellular response at low oxygen conditions in normal cells. Tumor cells adapt the hypoxia pathway to sustain at low oxygen tension.<sup>34,35</sup> Tumour hypoxia acts as a novel regulator of DNA methylation independently of HIF1A activity.<sup>36</sup> The results showed that methylated HIF1A is modified to differentially methylated HIF1A during the cellular transformation, where the HIF1A promoter undergoes partial demethylation due to the prevailing hypoxic conditions generated because of stress provided by non-adhesion for a period of 16h. HIF-1 transcription factor helps hypoxic cells to shift glucose metabolism from efficient oxidative phosphorylation to the less efficient glycolytic pathway to maintain their energy production (the Warburg effect).<sup>37</sup> A study demonstrated the relationship between *HIF1A* gene-altered expression and hypoxia in Bangladeshi breast cancer (BC) cases, revealing that HIF1A hypomethylation may contribute to its overexpression, promoting hypoxia-driven tumor progression in breast cancer.<sup>38</sup> Another study revealed that deregulated HIF-1α, due to DNA methylation and histone modifications, leads to esophageal cancer progression by driving cell cycle changes, angiogenesis, and radiotherapy resistance.<sup>39</sup> Significant overexpression of HIF1A in colon, breast, gastric, lung, skin, ovarian, pancreatic, prostate, and renal carcinomas were reported as an attractive target for prognosis and therapy.<sup>40-43</sup> These findings highlight the importance of methylated HIF1A as a potential non-invasive biomarker in oncology.

VEGF is a 40–45kDa homodimer protein secreted by various cells in physiologic and pathologic conditions. VEGF-A is a critical factor in modulating endothelial cell division, mitogenesis, cell migration, vasodilation, and vascular permeability. VEGF-A is upregulated

in tumors by both hypoxia-dependent and hypoxia-independent mechanisms.<sup>44</sup> VEGF-A binds to vascular endothelial growth factor receptor VEGFR1 or VEGFR2 and then activates downstream signals to promote angiogenesis.<sup>45</sup> In the present study, VEGFA is found to be unmethylated in both control and transformed cells, though the expression level was high in transformed cells.<sup>3</sup> Upon transplantation, unmethylated VEGFA was released into the circulation with a maximum intensity of 1.3547 in the 11<sup>th</sup> week, when tumor growth was initiated. However, methylated VEGFA is found to be responsible for its higher expression in colorectal cancer through the long non-coding RNA AK001058, required for angiogenesis promotion and ADAMTS12 (tumor suppressor disintegrin and metalloproteinase with thrombospondin motifs 12) down-regulation.<sup>46</sup> In addition, VEGFA is also regulated epigenetically by histone acetylation and DNA methylation in endometrial cancer.<sup>47</sup> It has been found to be a potential drug target in kidney renal clear cell carcinoma (KIRC).<sup>48</sup>

It was reported that during hypoxic conditions, the stable HIF-1α enhances glycolysis-related gene expression and further increases glycolysis in cancer.<sup>49,50</sup> HK2 is a phosphorylating enzyme responsible for the utilization of glucose in the intracellular environment. HK2 exerts cytoprotective effects in healthy and neoplastic cells and increases their efficiency in glucose usage.<sup>51</sup> Abnormal HK2 expression is observed in precancerous lesions<sup>52</sup> and may be considered as a predictive biomarker for HCC development.<sup>53</sup> The previous microarray data studies showed a 4.78 increased fold change of HK2 gene in transformed cells and no change in tumors when compared to normal cells. In continuation, unmethylated HK2 was released gradually in control mice from week 1 to 5 and declined in later weeks. In contrast, methylated HK2 was released in the circulation of tumorigenic mice from week 1 to 11, with maximum intensity at week 5. Studies showed that hypermethylation of the HK2 promoter at CpG island (HK2-CGI) may regulate HK2 expression and thereby influence the interaction between HIF 1α and HRE (hypoxia response element) during the process of tumorigenesis.

A similar methylation pattern was observed as a poor prognosis in hepatocellular carcinoma.<sup>54-56</sup>

EGFR is a transmembrane protein involved in activating downstream signal transduction pathways, including Raf1-extracellular signal-regulated kinase and PI3K/Akt, key in cell proliferation, cell growth, and inhibition of apoptosis. EGFR mutations, specifically Ex19del and exon 21 L858R, influence NSCLC progression and treatment response. Studies demonstrated that dacomitinib shows potential benefits in Indian patients with these mutations.<sup>57</sup> EGFR-targeting degraders, including Proteolysis-Targeting Chimeras (PROTACs), are emerging as potential strategies to overcome EGFR mutation-mediated resistance in NSCLC, addressing a critical unmet clinical need. Overexpression of EGFR or mutations in intracellular EGFR have been observed in 43% to 89% of cancers.<sup>58</sup> In our study, we observed the release of methylated EGFR in both control and tumorigenic mice from weeks 6 to 11. Minor variations in the intensities of bands may be responsible for increased EGFR expression to 2.43-fold in transformed cells and further decreased in tumors (as shown previously in the microarray data). Previous studies showed that in non-small-cell lung cancer (NSCLC), hypermethylation of the EGFR promoter is associated with reduced expression and inherent resistance to tyrosine kinase inhibitors (TKIs), whereas hypomethylation correlates with increased expression and enhanced treatment sensitivity.<sup>59</sup> Similarly, research on lung adenocarcinoma (LUAD) revealed that methylation of specific CpG sites in the EGFR promoter negatively correlates with transcription levels and protein expression, indicating a crucial regulatory role. Additionally, a positive association between promoter methylation and immune infiltration suggests that epigenetic alterations may influence the tumor microenvironment.<sup>60</sup> In metastatic colorectal cancer, EGFR hypermethylation correlates with poorer clinical responses, lower progression-free survival, and overall survival rates, further emphasizing the potential of methylation status as a predictive biomarker for treatment efficacy. Arginine-methylated EGFR (meEGFR) enhances ligand binding affinity and serves as a potential biomarker for predicting resistance to anti-EGFR therapy in metastatic colorectal cancer.<sup>61</sup> This data supports the role of EGFR modifications in cancer prognosis and highlights the importance of using methylations in non-invasive biomarker development.

DNA damage-inducible transcript 3 (DDIT3) is involved in various cellular processes, including apoptosis, differentiation, and stress response, and dysregulation leads to several diseases, including cancer.<sup>62,63</sup> We observed no change in the level of unmethylated DDIT3 in the circulation of both control and tumorigenic animals until week 5. Recent findings highlight the role of DDIT3 as a potential biomarker in CML, revealing that 66% of patients exhibit aberrant DDIT3 promoter methylation, which correlates positively with elevated white blood cell counts. DDIT3 acts as a transcriptional regulator by interacting with promoter regions of target genes, influencing gene expression through interactions with histone H3 lysine 27 (H3K27)-acetylated chromatin, thereby playing a crucial role in cellular stress responses, cell cycle arrest, and apoptosis.<sup>64,65</sup> DDIT3 has been a key regulator in T-cell infiltration and activation of fibroblast growth factor (FGF) signalling.<sup>66</sup>

We did not observe any amplification for HK2, EGFR, and DDIT3 in control and transformed cells, however released in the blood steam while generating tumors. Tough HIF1A in transformed cells did not enter into the circulation of tumorigenic mice (even in altered conditions like increased cycle number, annealing temperature, changing concentrations of primers, and lesser MgCl<sub>2</sub>).

However, observing the methylation status in transformed cells

and in the circulation of tumorigenic animal models strongly suggests that methylation mechanisms play a significant role in activating cancer pathways. The results demonstrated the important differences in the methylation status of genes while transforming from normal cells and while releasing into the circulation at early stages of cancer, indicating a strong association between transformation and tumor initiation and were comparable with the previous reports.<sup>67-69</sup> These findings provide crucial insights into the altered methylation status of specific genes driving cancer development and the application of these changes in developing DNA-based non-invasive biomarkers for early cancer detection. There might be limitations for the results to be applied in clinical use, and further study is needed to validate the findings.

## Conclusion

Based on the observations, we conclude that DNMTs play a major role in transforming the cells by altering the methylation patterns of the genome. Variation in the methylation pattern of HIF1A may induce the cells to transform by inducing a hypoxia-mediated pathway for their survival. Upon transplantation, the neoplastic cells at the tumor site release methylated HK2 and unmethylated VEGFA at the time / during tumorigenesis into the blood circulation, providing a clue in considering them as markers to detect cancer at an early stage.

## Ethical approval

The research was ethically approved by the ethical committee of CSIR-IICT, Hyderabad (IAEC; protocol number: IICT/08/2018).

## Acknowledgments

The authors acknowledge Acharya Nagarjuna University, Guntur-522510, Andhra Pradesh, and CSIR-Indian Institute of Chemical Technology, Hyderabad-500-007, Telangana, for their continuous support and encouragement.

Prof. Rajeswari Jinka to acknowledge Acharya Nagarjuna University for providing the Seed Money Grant No. ANU/CIIPR/26.5.2023, and RUSA 2.0 for providing the Research project of R&I No. RUSA-ANU/ANU/Research Project-02/2024, Mythreyi Jannu to acknowledge DST for providing DST-INSPIRE fellowship (IF200211).

## Conflicts of interest

The authors declare that there are no conflicts of interest.

## References

1. Senga SS, Grose RP. Hallmarks of cancer—the new testament. *Open Biol.* 2021;11(1):200358.
2. Hanahan D. Hallmarks of cancer: new dimensions. *Cancer Discov.* 2022;12(1):31–46.
3. Jinka R, Kapoor R, Pavuluri S, et al. Differential gene expression and clonal selection during cellular transformation induced by adhesion deprivation. *BMC Cell Biol.* 2010;11:93.
4. Zhang S, Xiao X, Yi Y, et al. Tumor initiation and early tumorigenesis: molecular mechanisms and interventional targets. *Signal Transduct Target Ther.* 2024;9(1):149.
5. Singh M, Kumar V, Sehrawat N, et al. Current paradigms in epigenetic anticancer therapeutics and future challenges. *Semin Cancer Biol.* 2022;83:422–440.
6. Urbano A, Smith J, Weeks RJ, et al. Gene-specific targeting of DNA methylation in the mammalian genome. *Cancers.* 2019;11(10):1515.
7. Geissler F, Nesic K, Kondrashova O, et al. The role of aberrant DNA methylation in cancer initiation and clinical impacts. *Ther Adv Med Oncol.* 2024;16:17588359231220511.

8. Baylin SB, Jones PA. A decade of exploring the cancer epigenome-biological and translational implications. *Nat Rev Cancer*. 2011;11(10):726–734.
9. Nikanjam M, Kato S, Kurzrock R. Liquid biopsy: current technology and clinical applications. *J Hematol Oncol*. 2022;15(1):131.
10. Wilkinson AL, Zorzan I, Gunn PJR. Epigenetic regulation of early human embryo development. *Cell Stem Cell*. 2023;30(12):1569–1584.
11. Zhu Y, Yang T, Wu Q, et al. Diagnostic performance of various liquid biopsy methods in detecting colorectal cancer: a meta-analysis. *Cancer Med*. 2020;9(16):5699–5707.
12. Jinka R, Kapoor R, Sistla PG, et al. Alterations in cell-extracellular matrix interactions during progression of cancers. *Int J Cell Biol*. 2012;2012:219196.
13. Jinka R, Pande G. Tumor model system useful to study multistage cancer. United States. 2015.
14. Kumar P, Nagarajan A, Uchil PD. Analysis of cell viability by the MTT assay. *Cold Spring Harb Protoc*. 2018;2018(6).
15. Dasari C, Yaghnam DP, Walther R, et al. Tumor protein D52 (isoform 3) contributes to prostate cancer cell growth via targeting nuclear factor- $\kappa$ B transactivation in LNCaP cells. *Tumour Biol*. 2017;39(5):1010428317698382.
16. Bo YY, Liang LD, Hua YJ, et al. High-purity DNA extraction from animal tissue using picking in the trizol-based method. *BioTechniques*. 2021;70(3):186–190.
17. Guha P, Das A, Dutta S, et al. A rapid and efficient DNA extraction protocol from fresh and frozen human blood samples. *J Clin Lab Anal*. 2018;32(1):e22181.
18. Limaye A, Cho K, Hall B, et al. Genotyping protocols for genetically engineered mice. *Curr Protoc*. 2023;3(11):e929.
19. Hattori N, Liu YY, Ushijima T. DNA methylation analysis. *Methods Mol Biol*. 2023;2691:165–183.
20. Zhu D, Li J, Zhang W, et al. Highly specific multiplex DNA methylation detection for liquid biopsy of colorectal cancer. *Clin Chim Acta*. 2025;565:120026.
21. Zhang P, Wu D, Zha X, et al. Glutamine promotes the proliferation of intestinal stem cells via inhibition of tp53-induced glycolysis and apoptosis regulator promoter methylation in burned mice. *Burns Trauma*. 2024;12:tkae045.
22. Ren L, Cheng SG, Kang PC, et al. Silenced LASP1 interacts with DNMT1 to promote TJP2 expression and attenuate articular cartilage injury in mice by suppressing TJP2 methylation. *Kaohsiung J Med Sci*. 2023;39(11):1096–1105.
23. Liu C, Tang H, Hu N, et al. Methylomics and cancer: the current state of methylation profiling and marker development for clinical care. *Cancer Cell Int*. 2023;23(1):242.
24. Fang Q, Yuan Z, Hu H, et al. Genome-wide discovery of circulating cell-free DNA methylation biomarkers for colorectal cancer detection. *Clin Epigenetics*. 2023;15(1):119.
25. Oliver J, Garcia-Aranda M, Chaves P, et al. Emerging noninvasive methylation biomarkers of cancer prognosis and drug response prediction. *Semin Cancer Biol*. 2022;83:584–595.
26. Goggins M. The role of biomarkers in the early detection of pancreatic cancer. *Fam Cancer*. 2024;23(3):309–322.
27. Mattox AK, Douville C, Wang Y, et al. The origin of highly elevated cell-free DNA in healthy individuals and patients with pancreatic, colorectal, lung, or ovarian cancer. *Cancer Discov*. 2023;13(10):2166–2179
28. Fattah S, Golpour M, Amjadi-Moheb F, et al. DNA methyltransferases and gastric cancer: insight into targeted therapy. *Epigenomics*. 2018;10(11):1477–1497.
29. Shen N, Du J, Zhou H, et al. A diagnostic panel of DNA methylation biomarkers for lung adenocarcinoma. *Front Oncol*. 2019;9:1281.
30. Esteller M, Dawson MA, Kadoch C, et al. The epigenetic hallmarks of cancer. *Cancer Discov*. 2024;14(10):1783–1809.
31. Vasishta S, Ammankallu S, Poojary G, et al. High glucose induces DNA methyltransferase 1 dependent epigenetic reprogramming of the endothelial exosome proteome in type 2 diabetes. *Int J Biochem Cell Biol*. 2024;176:106664.
32. Zhang J, Yang C, Wu C, et al. DNA methyltransferases in cancer: biology, paradox, aberrations, and targeted therapy. *Cancers*. 2020;12(8):2123.
33. Wang K, He Z, Jin G, et al. Targeting DNA methyltransferases for cancer therapy. *Bioorg Chem*. 2024;151:107652.
34. Agarwal AP, Kumar MS. Effect of epigenetic changes in hypoxia induced factor (HIF) gene across cancer types. *Gene*. 2025;934:149047.
35. Wicks EE, Semenza GL. Hypoxia-inducible factors: cancer progression and clinical translation. *J Clin Invest*. 2022;132(11):e159839.
36. Cimmino F, Avitabile M, Lasorsa VA, et al. HIF-1 transcription activity: HIF1A driven response in normoxia and in hypoxia. *BMC Med Genet*. 2019;20(1):37.
37. Chen Z, Han F, Du Y, et al. Hypoxic microenvironment in cancer: molecular mechanisms and therapeutic interventions. *Signal Transduct Target Ther*. 2023;8(1):70.
38. Islam MS, Jesmin. Exploring the correlation between hypoxia, HIF1A variants, and breast cancer in different ethnicities, and Bangladeshi women: through ELISA and integrative multi-omics analysis. *Biomark Insights*. 2024;19:11772719241278176.
39. Macedo-Silva C, Miranda-Gonçalves V, Henrique R, et al. The critical role of hypoxic microenvironment and epigenetic deregulation in esophageal cancer radioresistance. *Genes (Basel)*. 2019;10(11):927.
40. Jing X, Yang F, Shao C, et al. Role of hypoxia in cancer therapy by regulating the tumor microenvironment. *Mol Cancer*. 2019;18(1):157.
41. Mittal K, Kaur J, Sharma S, et al. Hypoxia drives centrosome amplification in cancer cells via HIF1 $\alpha$ -dependent induction of polo-like kinase 4. *Mol Cancer Res*. 2022;20(4):596–606.
42. Geng Y, Zheng X, Zhang D, et al. CircHIF1A induces cetuximab resistance in colorectal cancer by promoting HIF1 $\alpha$ -mediated glycometabolism alteration. *Biol Direct*. 2024;19(1):36.
43. Sabry D, El-Deek SEM, Maher M, et al. Role of miRNA-210, miRNA-21 and miRNA-126 as diagnostic biomarkers in colorectal carcinoma: impact of HIF-1 $\alpha$ -VEGF signaling pathway. *Mol Cell Biochem*. 2019;454(1–2):177–189.
44. Patel SA, Nilsson MB, Le X, et al. Molecular mechanisms and future implications of VEGF/VEGFR in cancer therapy. *Clin Cancer Res*. 2023;29(1):30–39.
45. Kang Y, Li H, Liu Y, et al. Regulation of VEGF-A expression and VEGF-A-targeted therapy in malignant tumors. *J Cancer Res Clin Oncol*. 2024;150(5):221.
46. Zheng S, Lin F, Zhang M, et al. Long non-coding RNA AK001058 regulates tumor growth and angiogenesis in colorectal cancer via methylation of ADAMTS12. *Am J Transl Res*. 2019;11(9):6117–6123.
47. Dou XQ, Chen XJ, Wen MX, et al. Alternative splicing of VEGFA is regulated by RBM10 in endometrial cancer. *Kaohsiung J Med Sci*. 2020;36(1):13–19.

48. Li X, Li M, Zhao T, et al. The discovery of promising candidate biomarkers in kidney renal clear cell carcinoma: evidence from the in-depth analysis of high-throughput data. *Am J Cancer Res.* 2023;13(9):4288–4304.
49. Cui N, Li L, Feng Q, et al. Hexokinase 2 promotes cell growth and tumor formation through the Raf/MEK/ERK signaling pathway in cervical cancer. *Front Oncol.* 2020;10:581208.
50. Ciscato F, Ferrone L, Masgras I, et al. Hexokinase 2 in cancer: A prima donna playing multiple characters. *Int J Mol Sci.* 2021;22(9):4716.
51. Lin J, Fang W, Xiang Z, et al. Glycolytic enzyme HK2 promotes PD-L1 expression and breast cancer cell immune evasion. *Front Immunol.* 2023;14:1189953.
52. Yu LR, Han XZ, Tang YZ, et al. Activation of the MEK/ERK pathway mediates the inhibitory effects of silvestrol on nasopharyngeal carcinoma cells via RAP1A, HK2, and GADD45A. *Front Biosci (Landmark Ed).* 2024;29(4):160.
53. Lee HG, Kim H, Son T, et al. Regulation of HK2 expression through alterations in CpG methylation of the HK2 promoter during progression of hepatocellular carcinoma. *Oncotarget.* 2016;7(27):41798–41810.
54. Lee NCW, Carella MA, Papa S, et al. High expression of glycolytic genes in cirrhosis correlates with the risk of developing liver cancer. *Front Cell Dev Biol.* 2018;6:138.
55. Wang X, Li L, Zhao K, et al. A novel LncRNA HITT forms a regulatory loop with HIF-1 $\alpha$  to modulate angiogenesis and tumor growth. *Cell Death Differ.* 2020;27(4):1431–1446.
56. Wang P, Zhao L, Gong S, et al. HIF1 $\alpha$ /HIF2 $\alpha$ -Sox2/Klf4 promotes the malignant progression of glioblastoma via the EGFR-PI3K/AKT signalling pathway with positive feedback under hypoxia. *Cell Death Dis.* 2021;12(4):312.
57. Batra U, Biswas B, Prabhash K, Krishna MV. Differential clinicopathological features, treatments and outcomes in patients with Exon 19 deletion and Exon 21 L858R EGFR mutation-positive adenocarcinoma non-small-cell lung cancer. *BMJ Open Respir Res.* 2023;10(1):e001492.
58. Shen J, Chen L, Liu J, et al. EGFR degraders in non-small-cell lung cancer: breakthrough and unresolved issue. *Chem Biol Drug Des.* 2024;103(4):e14517.
59. Fabrizio FP, Sparaneo A, Muscarella LA. Monitoring EGFR-lung cancer evolution: a possible beginning of a “methylation era” in TKI resistance prediction. *Front Oncol.* 2023;13:1137384.
60. Xu Z, Qin F, Yuan L, et al. EGFR DNA methylation correlates with EGFR expression, immune cell infiltration, and overall survival in lung adenocarcinoma. *Front Oncol.* 2021;11:691915.
61. Korphaisam K, Chou CK, Xia WY, et al. Arginine methylation of EGFR: a new biomarker for predicting resistance to anti-EGFR treatment. *Am J Cancer Res.* 2017;7(12):2587–2599.
62. Kunogi T, Konishi H, Sakatani A, et al. Probiotic-derived ferrichrome induces DDIT3-mediated antitumor effects in esophageal cancer cells. *Helyon.* 2024;10(6):e28070.
63. Hu H, Tian M, Ding C, et al. The C/EBP homologous protein (CHOP) transcription factor functions in endoplasmic reticulum stress-induced apoptosis and microbial infection. *Front Immunol.* 2019;9:3083.
64. Osman A, Lindén M, Österlund T, et al. Identification of genomic binding sites and direct target genes for the transcription factor DDIT3/CHOP. *Exp Cell Res.* 2023;422(1):113418.
65. Hazarika G, Kalita MJ, Kalita S, et al. Epigenetic modulation of DDIT3 and MGMT expression acts synergistically with resistance to imatinib towards CML disease progression: a hospital-based study. *Asian Pac J Cancer Prev.* 2023;24(12):4059–4069.
66. Yu X, Li W, Sun S, et al. DDIT3 is associated with breast cancer prognosis and immune microenvironment: an integrative bioinformatic and immunohistochemical analysis. *J Cancer.* 2024;15(12):3873–3889.
67. Barault L, Amatu A, Siravegna G, et al. Discovery of methylated circulating DNA biomarkers for comprehensive non-invasive monitoring of treatment response in metastatic colorectal cancer. *Gut.* 2018;67(11):1995–2005.
68. Gómez MG, Moran S, Cadena MP, et al. A new approach to epigenome-wide discovery of non-invasive methylation biomarkers for colorectal cancer screening in circulating cell-free DNA using pooled samples. *Clin Epigenetics.* 2018;10:53.
69. Qu Y, Zhang X, Qiao R, et al. Blood FOLR3 methylation dysregulations and heterogeneity in non-small lung cancer highlight its strong associations with lung squamous carcinoma. *Respir Res.* 2024;25(1):59.